Transportation Research Part B 42 (2008) 911–924

Contents lists available at ScienceDirect

Transportation Research Part B

journal homepage: www.elsevier.com/locate/trb

Robust optimal traffic signal timing

Yafeng Yin *

Department of Civil and Coastal Engineering, University of Florida, 365 Weil Hall, Box 116580, Gainesville, FL 32611, United States

ARTICLE INFO

Article history:
Received 22 May 2006
Received in revised form 4 March 2008
Accepted 17 March 2008

Keywords:
Pre-timed
Signal control
Traffic fluctuations
Robust timing

ABSTRACT

The performance of signal timings obtained by using conventional approaches for pre-timed control systems is often unstable under fluctuating traffic conditions. This paper presents three models to determine robust optimal signal timings that are less sensitive to fluctuations of traffic flows or perform better against the worst-case scenario without losing much optimality. Computational experiments are conducted to validate the model formulations and solution algorithms.

1. Introduction

While recent research has primarily focused on developing real-time adaptive signal control systems, the wide-scale implementation of such systems may be years away, particularly in developing countries, due to the associated high costs for implementation and maintenance. Because a big segment of signal controllers in use is still pre-timed (fixed-time or traffic-actuated), there is a significant need to further improve performances of those signal control systems (Smith et al., 2002).

Many of state-of-the-practice pre-timed systems are operated in a time-of-day mode in which a day is segmented into a number of time intervals, and a signal timing plan is predetermined for each time interval. Typically 3–5 plans are run in a given day. The basic premise is that the traffic pattern within each interval is relatively consistent and the predetermined timing plan is best suited for the condition of this particular time of day. The timing plan is often obtained by applying Webster's formula (Webster, 1958) or using optimization tools such as TRANSYT (Vincent et al., 1980) or TRANSYT-7F (Wallace et al., 1998), with the inputs of design flows, the mean values of traffic flows, for the time-of-day intervals.

However, real-world travel demands are intrinsically fluctuating, and traffic flows at intersections may vary significantly even for the same time of day and day of week. As an example, Fig. 1 displays hourly flows (including two-way right-, left-turn and through movements) at two crossing streets, 34th Street and University Avenue, in Gainesville, FL, during 9:00–11:00 a.m. on weekdays over a period of 3 months. The flows present significant day-to-day variations. Consequently an issue that traffic engineers may be confronted with is to determine what flows to use to optimize signal timings. This issue was hardly a concern in old days since the data collection used to be resource demanding, and traffic data were only collected for a couple of days. As the advancement of portable-sensor and telecommunications technologies make high-resolution traffic data more readily available, chances for traffic engineers to raise such a question become more prevalent.

* Tel.: +1 352 392 9537; fax: +1 352 392 3394.
E-mail address: yafeng@ce.ufl.edu

0191-2615/$ - see front matter © 2008 Elsevier Ltd. All rights reserved.
doi:10.1016/j.trb.2008.03.005

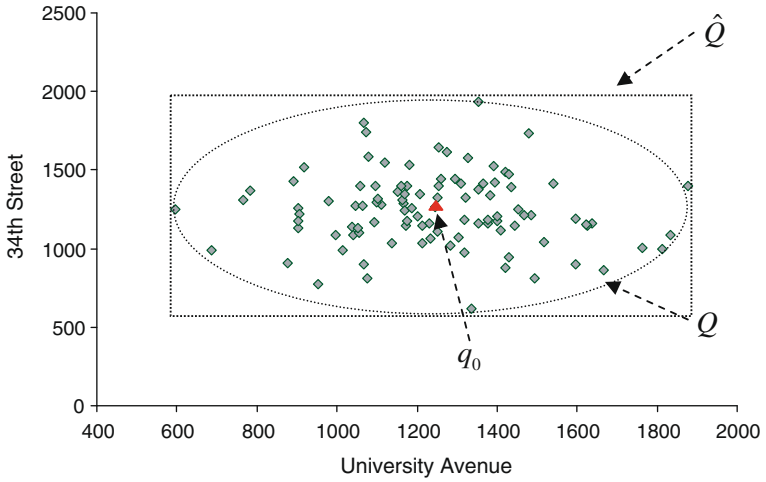

Fig. 1. Day-to-day AM-peak hourly flow rates at one intersection in Gainesville, FL.

This is particularly true in re-timing efforts for the closed-loop control systems with fiber optic connections. For example, in California, second-by-second returns of loop data can be obtained and archived via using AB3418 (The California legislature passed legislation, Assembly Bill 3418, requiring all signal controllers purchased in the state after January 1, 1996, to be compliant with a standardized communication protocol).

Use of the average flows (i.e., q^0 in Fig. 1) may not be a sensible choice. Heydecker (1987) pointed out that if the degree of variability of traffic flows is significant, optimizing signal timing with respect to the average flows may incur considerable additional delay, compared with the timing obtained by taking this variability into account. For small degree of variability, use of the average flows in conventional calculation methods will only lead to small losses in average performance (efficiency). However, as observed later in this paper, it may still suffer considerable losses in the performance against the worst-case scenarios or the stability of performance (robustness), thereby causing motorists' travel times unreliable. On the other hand, if the observations of highest flows are used instead, the resulting timing plans may be over-protective and unjustifiably conservative. The average performance (efficiency) is very likely to be inferior. Smith et al. (2002) suggested using 90th percentile volumes as the representative volumes to generate optimal timing plans and further advised that if time permits, other percentile volumes should be used to compare the results.

This paper intends to answer the question of what flows to use for signal optimization. More rigorously, this paper is to investigate methods of signal optimization for pre-timed control under demand fluctuations. In view of the conflicting nature of efficiency and robustness of signal control, a tradeoff would be inevitable to make. The paper attempts to develop a timing plan whose performance is near optimal in an average sense, and is fairly stable under any realization of uncertain traffic flows.

Such a timing plan also allows a slower deterioration of performance. We note that the signal timing process is normally time-consuming, and thus it is rarely repeated unless changes in traffic conditions are so significant that the system begins performing poorly. It has been estimated that traffic experiences an additional 3–5% delay per year as a consequence of not retiming signals as the conditions evolve over time (Luyanda et al., 2003). Therefore, it would be more desirable to have timing plans that accommodate or tolerate these changes in traffic to a great extent.

Since the seminal work of Webster (1958), significant efforts have been devoted to improving signal timing for saturated isolated intersections, coordinated arterials and grid networks, etc. (see, e.g., Gazis, 1964; Robertson and Bretherton, 1991 and Gartner, 2002). However, only a few studies have been conducted to address signal timing under flow fluctuations for pre-timed control systems. Heydecker (1987) investigated the consequences of variability in traffic flows and saturation flows for the calculation of signal settings and then proposed an optimization formulation that minimizes the mean rate of delay over the observed arrivals and saturation flows. Following the same notion, Ribeiro (1994) proposed a novel technique called Grouped Network for using TRANSYT to calculate timing plans that are efficient even when demand is variable.

In this paper, we present three models to determine robust optimal signal timings that minimize the mean of delays per vehicle under day-to-day demand fluctuations as well as maintain a fairly stable performance under those fluctuations or perform better against the worst-case or high-consequence scenarios. These three approaches are simple in structure, and tractable in computation. We demonstrate these approaches on isolated fixed-time signalized intersections, but the principles and methodology involved are applicable more widely, and can be applied to fixed-time or actuated controls[1] for arterials and grid networks.

[1] Although actuated signals can respond to traffic fluctuations to a certain degree, the underlying timing plan still plays an important role in the determining the efficiency and robustness of the control, especially, over a coordinated semi-actuated signal-controlled arterial.

For the remainder, Section 2 introduces a scenario-based mean-variance signal optimization model, and briefly discusses its properties and solution algorithm. Section 3 formulates another scenario-based model to minimize the conditional value-at-risk of the loss associated with a signal timing plan. Section 4 presents a min–max model as well as its solution algorithm. Section 5 applies these three models to two four-stage fixed-time isolated intersections, and then uses Monte-Carlo simulations to validate the models. Conclusions and recommendations for further research are offered in the last section.

2. Scenario-based mean-variance optimization

The scenario-based mean-variance model is a straightforward extension to the principles developed in Heydecker (1987) and Ribeiro (1994). The model represents uncertainty of traffic flows via a limited number of discrete flow scenarios associated with strictly positive probability of occurrence, and then attempts to optimize signal timings across these scenarios for solutions that are near-optimal and robust with respect to the population of all possible realizations of uncertainty. The concept has been discussed extensively in Mulvey et al. (1995), and has been applied to different domains, such as finance, electric utilities and telecommunications (e.g., Laguna, 1998).

2.1. Model formulation

Without loss of generality, we consider an isolated fixed-time signalized intersection. To represent the uncertainty of traffic flows to the intersection, a set of scenarios $\Omega = \{1,2,3,\ldots,K\}$ is introduced. For each scenario $k \in \Omega$, the probability of occurrence is π^k, the traffic flow at lane group i is q_i^k. Given a signal timing plan and a flow scenario k, in order to allow for transient surges of traffic flows, we use the delay equation in Highway Capacity Manual (HCM) (TRB, 2000) to estimate the delay per vehicle,

$$d(q^k, C, g) = \frac{\sum_{i=1}^{N}\left[\frac{C(1-\lambda_i)^2 q_i^k}{2(1-\lambda_i \min(1, x_i^k))} + 900Tq_i^k\left(x_i^k - 1 + \sqrt{(x_i^k-1)^2 + \frac{4x_i^k}{c_i T}}\right)\right]}{\sum_{i=1}^{N} q_i^k} \tag{1}$$

where $d(q^k,C,g)$ denotes the delay per vehicle (s) and we sometimes simplify it as d^k; C is the cycle length (s) and g denotes the vector of effective green time for each lane group;N is the number of lane groups; λ_i is effective green split for lane group i and $\lambda_i = g_i/C$; x_i^k represents the degree of saturation for lane group i under flow scenario k, equal to $q_i^k/\lambda_i s_i$ and s_i is the saturation flow for the lane group i (veh/h); T is the duration of analysis period, e.g., 0.25 h, and c_i is the capacity for lane group i (veh/h), equal to $\lambda_i s_i$. The above delay equation is continuous, but neither convex nor differentiable (due to the minimum operator). Note that other delay formulae can be applied as well. Dion et al. (2004) compared several methods for delay estimates at fixed-time signalized intersections, and concluded that the equations defined in 1997 HCM, 1995 Canadian Capacity Guide, and 1981 Australian Capacity Guide and INTEGRATION microscopic simulation produce consistent results under both under-saturated and over-saturated conditions.

Given a set of flow scenarios, we now seek for a robust signal timing plan that minimizes the mean of delays per vehicle across all of the scenarios as well as minimizes the variability of the performance. Since these two objectives conflict with each other, a tradeoff is needed. In this paper we use standard deviation (SD) to represent the variability of performance, i.e., a measure of robustness, and then establish a mean–SD tradeoff. The scenario-based optimization model for determining the cycle length and green times is shown below:

MSD :

$$\min_{g,C} \quad Z = (1-\gamma)\sum_{k\in\Omega}\pi^k d^k + \gamma\sqrt{\sum_{k\in\Omega}\pi^k (d^k - \sum_{k\in\Omega}\pi^k d^k)^2} \tag{2}$$

subject to linear constraints on g and C

where γ is a weighting parameter, $0 \leqslant \gamma \leqslant 1$.

It is easy to see that the first component of the objective function (Eq. (2)) is the mean of the delays per vehicle across all of flow scenarios while the second represents the SD of the delays per vehicle. The parameter γ reflects the tradeoff between mean (efficiency) and SD (stability), varying from zero (minimizing the mean only) to one (minimizing the SD only). Note that when γ equals zero, the above problem is equivalent to the model developed in Heydecker (1987).

2.2. Discussions for model implementation

2.2.1. Solution algorithm

Note that Eq. (2) is continuous, and the feasibility set defined by linear constraints on g and C is non-empty, closed and bounded. According to Weierstrass' Theorem (e.g., Bazaraa et al., 1993), there exists an optimal solution to the optimization problem. However, since Eq. (2) is non-convex and non-differentiable, it may be difficult to obtain a global optimum. Despite this, the simple structure of the problem (linear constraints only) allows many existing algorithms to solve efficiently for local optima, which often serve well the purpose for engineering applications. A sequential quadratic programming (SQP)

subroutine with finite-differencing derivatives in Matlab is used in this paper to solve the MSD problem. Because the solver can only provide local optimal solutions, we solve the problem multiple times, each time with a different randomly generated initial solution. The best local optimal solution is taken as the final solution.

2.2.2. Scenarios

There is no doubt that the scenarios in Ω are only one possible set of realizations of the uncertain traffic flows. Two important questions about the scenario-based robust optimization are: (1) how many scenarios should be included in order to find a solution that is robust across the population of all possible realizations of uncertainty and (2) how to specify these scenarios and their associated probabilities. Intuitively, the more scenarios we include, the more robust solution we are likely to obtain. However, as the number of scenarios increases, the problem may become prohibitively large. Fortunately, prior studies (e.g., Mulvey et al., 1995 and Laguna, 1998) have shown, confirmed by our computation experiments, that relatively small number of scenarios will be able to produce near-optimal policies. In regard to the other question, as Mulvey et al. (1995) pointed out importance sampling in stochastic simulation can be applied to generate the representative scenarios, if the distributions are known. For real-world applications where the distributions of flows are normally unknown, we suggest selecting 20–200 flow scenarios from the field data for the same time-of-day interval, with assuming equal probability of occurrence. The observations of flows can be sorted by their resulting saturation degrees, and then flow scenarios can be determined as observations in the appropriate percentiles.

2.2.3. Choice of weighting parameter

The weighting parameter γ represents the tradeoff between efficiency and robustness. Our computation experiments show that although a large value of γ leads to more robust signal control, the average performance is far from optimal. If traffic engineers favor efficiency over robustness, smaller values may be used, presumably between 0 and 0.5. Certainly if time permits, a series of values can be used to create a frontier of non-dominated solutions, from which a compromised solution can be determined through a decision-making process.

3. Scenario-based conditional value-at-risk minimization

3.1. Conditional value-at-risk

The MSD model uses the SD of delays per vehicle to measure the robustness of a signal timing plan. However, travelers and system managers may be more concerned with the adverse system performance, and are less likely to complain if the delay is less than expected. The SD measure however does not account for this asymmetric effect and is indifferent to the deviations above and below the mean. Considering it may be desirable to have a timing plan that performs reasonably well against high-consequence scenarios, we minimize the expected loss or regret (to be defined) incurred by those high-consequence scenarios whose collective probability of occurrence is $1-\alpha$, where α is a specified confidence level (say, 90%). In financial engineering, the performance measure is known as conditional value-at-risk (CVaR), or mean excess loss (Rockafellar and Uryasev, 2002). Fig. 2a illustrates the concept of CVaR. The probability density function and mass function of a continuous loss are shown in the figure. The area of the shade under the density function is $1-\alpha$, and the CVaR is simply the mean of the losses located in the shaded area.

We now define the loss function. For each flow scenario $k \in \Omega$, the following optimization problem can be solved for the minimum delay per vehicle with respect to that scenario, denoted as d_k^*,

$$d_k^* = \min_{C,g} d(C,g,q^k) \quad \text{subject to linear constraints on } g \text{ and } C \tag{3}$$

Consequently, for any timing plan (C,g) that may not be optimal for scenario k, the loss or regret can be defined as

$$L_k = d(C,g,q^k) - d_k^* \quad \forall k \tag{4}$$

where L_k is the loss or regret of the timing plan (C,g) associated with scenario k, and d_k is computed using Eq. (1). Assuming that the loss is ordered as $L_1 < L_2 < \cdots < L_K$, let k_α be the unique index such that

$$\sum_{k=1}^{k_\alpha} \pi_k \geqslant \alpha > \sum_{k=1}^{k_\alpha - 1} \pi_k \tag{5}$$

In words, L_{k_α} is the maximum loss that is exceeded only with probability $1-\alpha$, called as α-value-at-risk (α-VaR). Consequently, the expected loss exceeding the α-VaR, i.e., CVaR, is

$$\phi_\alpha = \frac{1}{1-\alpha}\left[\left(\sum_{k=1}^{k_\alpha} \pi_k - \alpha\right)\cdot L_{k_\alpha} + \sum_{k=k_\alpha+1}^{K} \pi_k L_k\right] \tag{6}$$

The second component in the bracket is simply to compute the mean value exceeding the α-VaR, and the first is to split the probability 'atom' at the loss point L_{k_α} to make the collective probability of scenarios considered in the bracket exactly equal $1-\alpha$. See Fig. 2b for an illustration of the concept. It can be seen that the probability mass function has a jump at the loss

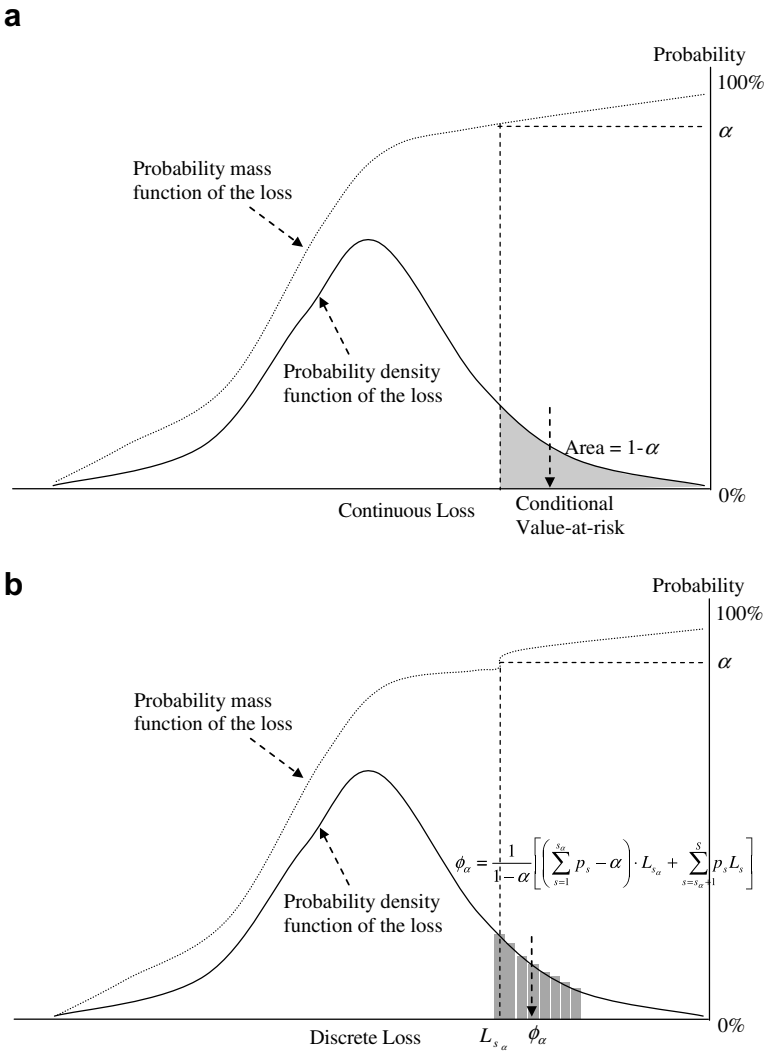

Fig. 2. Illustration of concept of CVaR.

point L_{k_α} due to the associated probability of π_{k_α}. To make the collective probability of scenarios exactly equal to $1-\alpha$, we need to split the probability.

3.2. Model formulation

For each signal timing plan, Eq. (6) can be used to compute the CVaR, and our intention is to find a plan that leads to the minimum CVaR. Rockafellar and Uryasev (2002) showed that minimizing Eq. (6) is equivalent to solving the following minimization problem:

$$\min_{C,g,\xi} Z_\alpha = \xi + \frac{1}{1-\alpha}\sum_{k=1}^{K}\pi_k \cdot \max(L_k(C,g) - \xi, 0) \tag{7}$$

where ξ is a free decision variable. It can be proved that the optimal value of (7) is the minimum CVaR, and the solution (C,g) is the optimal robust timing plan. Consequently, the robust signal timing optimization model can be formulated as follows:

MCVAR :

$$\min_{C,g,\xi} Z_\alpha = \xi + \frac{1}{1-\alpha}\sum_{k=1}^{K}\pi_k \cdot \max(d(C,g,q^k) - d_k^* - \xi, 0) \tag{8}$$

subject to linear constraints on g and C

Although the MCVAR problem is a non-convex and non-differentiable optimization problem (due to the delay function), it has a simple structure as well. Note that the objective function is convex with respect to ξ and d_k^* is predetermined by solving the optimization problem (3). Therefore the complexity of the MCVAR problem is comparable to the MSD problem. Compared with directly minimizing α-VaR, such a formulation offers computational advantages and allows handling a large number of scenarios, which has been demonstrated by previous studies in portfolio optimization (e.g., Krokhmal et al., 2002), facility location (e.g., Chen et al., 2006) and freeway service patrol fleet allocation (Yin, in press). This paper uses a SQP subroutine with finite-differencing derivatives in Matlab to solve the formulation.

We further note that a variant of the MCVAR problem can be formulated to minimize directly the average delay with incorporating a CVaR constraint.

4. Min–max optimization

One of the major drawbacks of the scenario-based approach is the additional efforts required to specify the scenarios. Moreover, as the number of scenarios increases, the problem may become computationally demanding. Here we apply robust optimization to determine a robust optimal timing plan.

The key point is that uncertain traffic flows are assumed to be bounded by a likelihood region. To specify the region, traffic engineers only need to provide their estimates of maximum and minimum likely flows for each lane group (denoted as $q_i^{\max}$ and $q_i^{\min}$, respectively). Within the region, we then seek for robust timing plans that tolerate changes in traffic flows up to the given bound. More specifically, we optimize the signal timing against the worst-case scenario realized within the region. It will be shown later that by selecting an appropriate geometry of the region, we can avoid being either careless (without considering variability of flows at all) or overly conservative. Consequently we will obtain a timing plan that is less sensitive to the fluctuations of traffic flows without losing much optimality.

We further note that the robust optimization approach is also attractive in situations where agencies do not have enough resources to do a meaningful data collection but have some prior knowledge about traffic conditions of the intersections. As shown later in the paper, even if the specified maximum and minimum flows are biased, the robust timing approach is able to produce reasonably good and stable timing plans.

The above concept is the basic notion behind a stream of recent research in the area of robust optimization (see Ben-Tal and Nemirovski, 2002 for an overview). Successful applications of robust optimization can be found in areas such as finance, telecommunication and structural engineering (e.g., Ben-Tal and Nemirovski, 1999).

4.1. Likelihood region of flows

The geometry of the flow likelihood region actually reflects preference or tradeoff that traffic engineers may have between efficiency and robustness. It may be straightforward to assume that traffic flow of each lane group independently varies within the interval of $Q_i = [q_i^{\min}, q_i^{\max}]$. When combined together, the whole likelihood region becomes $\widehat{Q} = Q_1 \times Q_2 \times \cdots \times Q_N$. $\widehat{Q}$ is a box centered at the nominal (average) traffic flows $q^0 \in R^N$, a vector with elements of $(q_i^{\max} + q_i^{\min})/2$. See Fig. 1 for an illustration. Since we attempt to optimize signal timing against the worst-case scenario, the corresponding flows would be the one with the highest arrival $q_i^{\max}$ for each lane group. Obviously it is too conservative, because in the real world it is rare that all lane groups experience their corresponding highest flows simultaneously.

Instead, we use the following ellipsoidal region to confine traffic arrivals at intersections:

$$Q = \{q \in R^N \,|\, q = q^0 + M \cdot u,\ \|u\|_2 \leqslant 1\} \tag{9}$$

where $M \in R^{N \times N}$, a diagonal matrix with elements of $\theta \cdot (q_i^{\max} - q_i^{\min})/2$. The region can be also written as

$$Q = \left\{ q \in R^N \left| \sum_{i=1}^{N} \left(\frac{q_i^{\max} - q_i^{\min}}{2} \right)^{-2} \cdot (q_i - q_i^0)^2 \leqslant \theta^2 \right. \right\} \tag{10}$$

θ is a parameter, reflecting attitudes of traffic engineers towards robustness. The larger is θ, the more preference to robustness. When $\theta = 0$, Q contains q^0 only, suggesting that the signal timing is optimized with respect to the nominal flow, the conventional approaches. When $\theta = 1$, Q would be the largest volume ellipsoid contained in the box region $\widehat{Q}$ specified above (see Fig. 1).

The choice of likelihood region will affect the optimality and robustness of the resultant timing plan. The ellipsoidal region is much more realistic than the box region in the sense that not all lane groups achieve their corresponding highest flows at the same time. However, with an ellipsoidal likelihood region, it is not straightforward to identify the worst-case flow vector, and the vector could be different for different signal settings. It should be stressed that when applying the min–max concept, we do not intend to incorporate all the possible realizations of traffic flows into the likelihood region. The minimum or maximum flows by no means are the least or highest possible realizations of uncertain flows. Instead, the choice of the region should make the resulting model computationally tractable and reflect the decision maker's attitude toward risk. Compared with the traditional approach where the timing is optimized against a single scenario, optimization against a region is expected to generate a more robust solution, even that the region does not represent the support of the demand distributions (Ben-Tal and Nemirovski, 1999).

4.2. Model formulation

Within the likelihood region of traffic flows, we seek for a robust timing plan that minimizes the delay per vehicle under the worst-case demand scenario bounded by the likelihood region. Mathematically, the robust optimal signal timing for an isolated fixed-time signal can be obtained by solving the following min–max optimization problem:

$$\begin{aligned} &\text{MNMX}: \\ &\min_{C,g} \max_{q\in Q} d(C,g,q) \\ &\text{subject to linear constraints on } g \text{ and } C \end{aligned} \tag{11}$$

In Eq. (11), the decision variables for the minimization problem are the cycle length and effective green times, and the maximization problem is to determine the worst-case flow vector. Essentially the objective function is to minimize the maximum delay per vehicle possibly incurred within the likelihood region. To motivate the solution algorithm, the MNMX is re-written equivalently as follows:

$$\begin{aligned} &\text{MNMX}: \\ &\min_{C,g,y} y \\ &\text{subject to } d(C,g,q) \leqslant y \quad \forall q \in Q \text{ and other linear constraints on } g \text{ and } C \end{aligned} \tag{12}$$

4.3. Solution algorithm

There is no readily-available solution algorithm for the above min–max problem. Below we propose a cutting-plane solution algorithm (see, e.g., Bazaraa et al., 1993). The algorithm generates the worst-case flow vectors one a time, each of which produces a constraint that cuts away part of the region not feasible to the original problem. Mathematically, the algorithm can be stated as follows:

Step 0: (Initialization) Choose an initial timing plan $g^{(1)}$ and set the iteration counter, n to 1.
Step 1: Given $g^{(n)}$, solve the following (sub) problem:

$$q^{(n)} = \arg\max_{q} \left\{ d(C^{(n)}, g^{(n)}, q) : \ q \in Q \right\} \tag{13}$$

Step 2: Using $q^{(1)}, \ldots, q^{(n)}$ generated in Step 1, formulate and solve the following (master) problem:

$$\begin{aligned} &(C^{(n+1)}, g^{(n+1)}, y^{(n+1)}) = \arg\min_{(g,C,y)} y \\ &\text{subject to linear constraints on } g \text{ and } C \text{ and } d(C,g,q^{(k)}) \leqslant y, \quad k = 1,2,\ldots,n \end{aligned} \tag{14}$$

Step 3: If $\max_i(|g_i^{(n+1)} - g_i^{(n)}|) \leqslant \delta$, then stop, where δ is a predetermined error tolerance (e.g., 1 s). Otherwise, let $n = n + 1$, go to Step 1.

At the current timing plan $g^{(n)}$, the subproblem in Step 1 finds the flow vector $q^{(n)}$ that yields the maximum delay per vehicle. The subproblem is a quadratically-constrained problem, which can be solved efficiently by using an iterative descent scheme. At each iteration, a localized linear approximation can be formulated using the finite-differencing derivatives: $\max_{\|u\|\leqslant 1} \nabla d_q^{\mathrm{T}} \cdot M \cdot u$, where ∇d_q is the vector of derivatives of the delay per vehicle with respect to traffic flows. The optimal solution of this quadratic problem is $M \cdot \nabla d_q / \sqrt{(M \cdot \nabla d_q)^{\mathrm{T}} \cdot (M \cdot \nabla d_q)}$.

The master problem in Step 2 finds the timing plan $g^{(n+1)}$ that minimizes the maximum delay per vehicle among n flow vectors $q^{(1)}, \ldots, q^{(n)}$. The problem is essentially a relaxation of the MNMX problem and can be solved efficiently by a SQP algorithm with finite-differencing derivatives.

The proposed algorithm essentially solves a sequence of two nonlinear programming problems. Therefore, the computation effort for obtaining robust signal timings only increases in a polynomial manner. Note that the proposed algorithm is not totally heuristic. Assume that both $q^{(n)}$ and $(g^{(n+1)}, C^{(n+1)}, y^{(n+1)})$ globally solve the problems of (13) and (14) in Steps 1 and 2, respectively, and (g^*, C^*, y^*) is a global optimal solution to the MNMX problem. Because the problem of (14) is a relaxation of the MNMX problem, we have $y^{(n+1)} \leqslant y^*$. If the above algorithm stops at some finite iteration n, then $g^{(n+1)} = g^{(n)}$, and we have $y^{(n+1)} \geqslant d(C^{(n+1)}, g^{(n+1)}, q^{(n)}) = \max_{q\in Q} d(C^{(n+1)}, g^{(n+1)}, q)$, which implies that $(g^{(n+1)}, C^{(n+1)}, y^{(n+1)})$ is a feasible solution to the MNMX problem. When combined with $y^{(n+1)} \leqslant y^*$, the optimality of (g^*, C^*, y^*) implies that $y^{(n+1)} = y^*$, i.e., $(g^{(n+1)}, C^{(n+1)}, y^{(n+1)})$ is optimal to the MNMX problem. When the algorithm generates an infinite sequence, it can be further proved that any of its subsequential limits is optimal to the MNMX problem. The proof is similar to the one in Yin and Lawphongpanich (2007). The convergence proof relies on the assumption that the problems of (13) and (14) can be solved globally. Since both problems are non-convex, in practice the problems may be solved multiple times with different initial solutions for a better local optimum. Our computation experiments show that it normally takes less than 10 iterations for the algorithm to converge.

5. Numerical examples

5.1. Example 1

We apply the proposed approaches to an isolated fixed-time four-stage signalized intersection. The input data are shown in Table 1 for both under-saturated and over-saturated conditions (under the maximum flows). We use the NEMA phasing convention to represent intersection movements with 1, 3, 5, 7 for left-turn and 2, 4, 6, 8 for through and right-turn movements (National Electrical Manufacturers Association, 1989). A specific lead-lag phasing sequence is used in the example, and the resulting constraints for the MSD, MCVAR and MNMX problems are:

$$g_1 + g_2 + g_3 + g_4 + L = C \tag{15}$$

$$g_1 = g_6, \quad g_2 = g_5, \quad g_3 = g_8, \quad g_4 = g_7 \tag{16}$$

$$g_i \geqslant g_{\min}, \quad i = 1, 2, \ldots, 8 \tag{17}$$

$$C_{\min} \leqslant C \leqslant C_{\max} \tag{18}$$

where L is the total lost time per cycle, 14 s used in the example; $g_{\min}$ is minimum green time, 8 s used, and $C_{\min}$ and $C_{\max}$ are the minimum and maximum cycle length, specified as 50 and 140 s, respectively. When using Eq. (1) to calculate the delay, the duration of analysis period is set as 0.25 h.

The computation experiments are conducted as follows:

5.1.1. Signal timing optimization

For the scenario-based MSD and MCVAR models, 2000 flow samples are first generated assuming that traffic flows follow normal distributions with means and SDs reported in Table 1. These 2000 samples serve as the observations from the field, and are then sorted by their saturation degrees. Flow scenarios are determined as samples in the appropriate percentiles with equal probability of occurrence. Different numbers of scenarios are tested in the computation experiments. For the MSD model, a series of value of γ are used to reflect different attitudes towards robustness and efficiency. Tables 2 and 4 report selected plans resulted by using 500 scenarios and γ equal to 0.0 or 0.5 (indicated as MSD-0.0 and MSD-0.5). For the MCVAR model, α is set to be 90% to represent the confidence level, and the resulting timing plan is denoted as MCVAR-90%.

For the MNMX model, the minimum and maximum flows in Table 1 are specified (the interval is approximately the 95% confidence interval, if flows follow normal distribution specified as above). Given the minimum and maximum flows, the

Table 1
Input data

Lane group	Saturation flow rate	Under-saturated				Over-saturated			
		Scenario-based		Min–Max		Scenario-based		Min–Max	
		Average flow	SD of flows	Minimum flow	Maximum flow	Average flow	SD of flows	Minimum flow	Maximum flow
1	1900	225	65	100	350	275	90	100	450
2	3800	400	100	200	600	525	140	250	800
3	3800	650	125	400	900	875	160	550	1200
4	1900	275	65	150	400	275	60	150	400
5	1900	250	25	200	300	350	75	200	500
6	3800	500	100	300	700	650	175	300	1000
7	3800	650	75	500	800	900	150	600	1200
8	1900	170	25	120	220	250	65	120	380
Saturation degree	–	0.59	–	0.39	0.82	0.80	–	0.47	1.13

Table 2
Resulting timing plans (under-saturated)

Lane group	1	2	3	4	5	6	7	8	Cycle length
Average	9	9	11	11	9	9	11	11	54
MNMX-0.5	10	9	13	12	9	10	12	13	59
MNMX-1.0	13	11	16	14	11	13	14	16	68
MSD-0.0	11	10	14	13	10	11	13	14	62
MSD-0.5	13	11	16	15	11	13	15	16	68
MCVAR-90%	13	12	16	15	12	13	15	16	70
75th percentile	9	9	13	13	9	9	13	13	59
90th percentile	9	12	14	15	12	9	15	14	64
100th percentile	16	13	18	18	13	16	18	18	79

MNMX model is solved with values of θ varying from 0 to 1. Tables 2 and 4 report two selected plans with θ equal to 0.5 or 1.0 (indicated as MNMX-0.5 and MNMX-1.0).

For the purpose of comparisons, we also use the average flows, 75th, 90th and 100th percentile flows from the generated samples to optimize the signal settings using conventional optimization methods. More specifically, the timing plans are calculated by solving the following problem:

$$\min_{C,g} d(C,g,q^i) = \frac{\sum_{i=1}^{8}\left[\frac{C(1-\lambda_i)^2 q_i}{2(1-\lambda_i \min(1,x_i))} + 900Tq_i(x_i - 1 + \sqrt{(x_i-1)^2 + \frac{4x_i}{c_i T}})\right]}{\sum_{i=1}^{8} q_i} \tag{19}$$

subject to constraints (15)–(18)

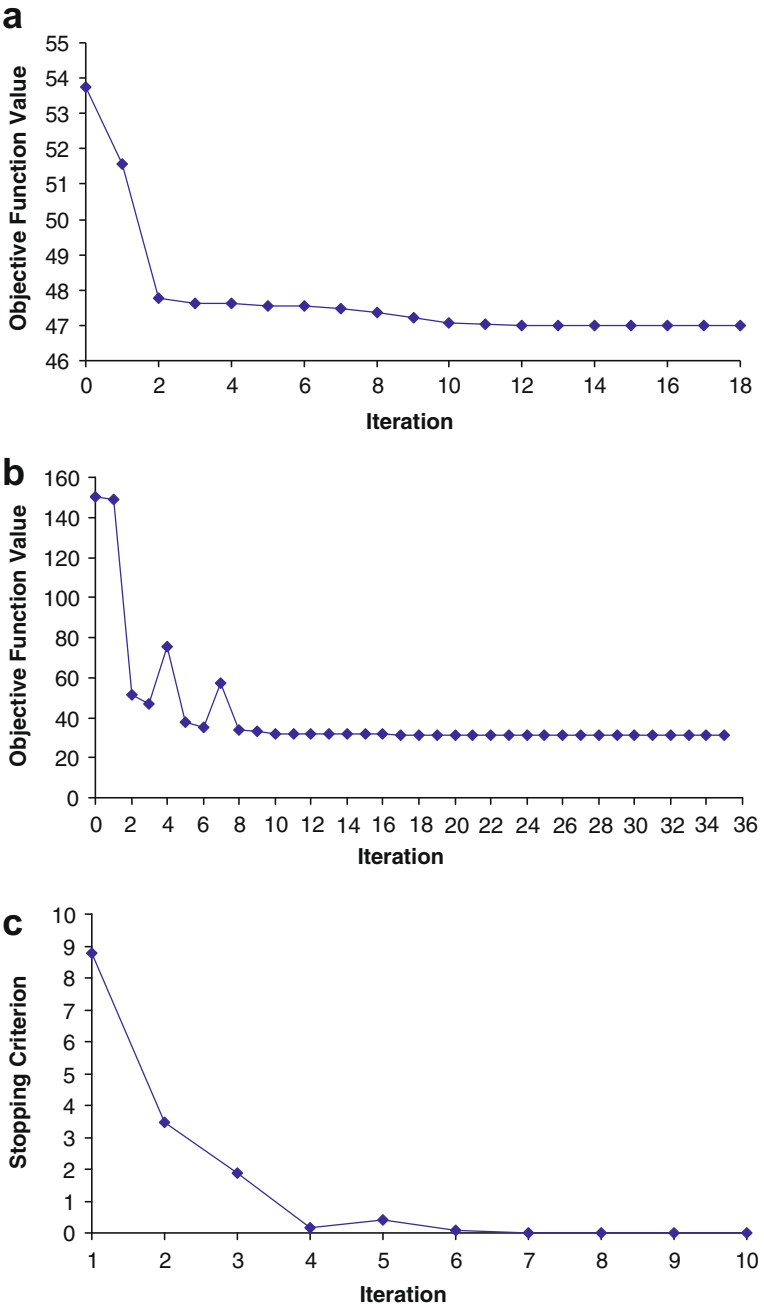

Fig. 3. Convergence plots for solving robust signal timing models.

Tables 2 and 4 report the resulting timing plans for both under-saturated and over-saturated cases. The plans appear quite different from each other. Fig. 3 is the typical convergence plots for solving the proposed models. In all computational experiments, the algorithms converge very quickly.

5.1.2. Monte-Carlo simulation

The efficiency and robustness of the resultant timing plans are tested by a macroscopic Monte-Carlo simulation, which is intended to replicate the real-world traffic conditions. Samples of traffic flows are drawn from normal distributions with means and SDs reported in Table 1, and for each sample the delay per vehicle resulted by each timing plan (reported in Tables 2 and 4) is computed using Eq. (1). After drawing 5000 samples, the mean, SD, maximum and the 90th percentile of delays per vehicle and the 90%-conditional-value-at-risk of the loss incurred by all samples are calculated for each timing plan, and are reported in Tables 3 and 5.

By examining Tables 3 and 5, it is interesting to observe that:

- The plan optimized against the average flows presents a good average performance. This observation is consistent with the conclusion made in Heydecker (1987) that for small degrees of variability use of mean values in conventional calculation methods will lead only to small loss in efficiency.

Table 3
Comparisons of timing plans via Monte-Carlo simulation (under-saturated)

	Mean of delays per vehicle	SD of delays per vehicle	Worst-case delays per vehicle	90th percentile delays per vehicle	90% CVaR of loss	Change (%)				
						Mean	SD	Worst	90th	CVaR
Average	37.2	7.7	92.2	47.0	17.0	–	–	–	–	-
MNMX-0.5	36.3	5.5	75.0	43.3	12.0	−2.3	−28.3	−18.6	−7.8	−29.4
MNMX-1.0	36.8	4.2	66.3	42.2	10.8	−1.0	−44.7	−28.1	−10.3	−36.6
MSD-0.0	35.9	5.3	80.0	42.6	11.1	−3.3	−30.9	−13.2	−9.3	−35.0
MSD-0.5	36.4	4.3	73.1	41.6	9.9	−2.2	−43.7	−20.7	−11.5	−42.1
MCVAR-90%	36.6	4.2	73.2	41.7	9.9	−1.5	−45.2	−20.6	−11.2	−42.1
75th percentile	37.5	6.8	84.7	46.1	16.5	0.8	−11.2	−8.1	−1.9	−3.4
90th percentile	39.9	8.8	100.1	51.6	23.5	7.4	14.8	8.6	9.8	37.7
100th percentile	38.4	4.1	79.6	43.0	11.9	3.2%	−46.7%	−13.6%	−8.4%	−30.1%

Table 4
Resulting timing plans (over-saturated)

Lane group	1	2	3	4	5	6	7	8	Cycle length
Average	16	15	21	21	15	16	21	21	87
MNMX-0.5	20	18	25	25	18	20	25	25	102
MNMX-1.0	24	19	29	29	19	24	29	29	116
MSD-0.0	19	18	23	24	18	19	24	23	99
MSD-0.5	22	19	27	27	19	22	27	27	109
MCVAR-90%	22	18	25	26	18	22	26	25	105
75th percentile	30	17	25	23	17	30	23	25	108
90th percentile	20	17	29	33	17	20	33	29	114
100th percentile	25	21	39	40	21	25	40	39	139

Table 5
Comparisons of timing plans via Monte-Carlo simulation (over-saturated)

	Mean of delays per vehicle	SD of delays per vehicle	Worst-case delays per vehicle	90th percentile delays per vehicle	90% CVaR of loss	Change (%)				
						Mean	SD	Worst	90th	CVaR
Average	76.7	20.7	183.7	105.1	36.3	–	–	–	–	–
MNMX-0.5	76.0	18.4	169.4	101.6	33.2	−0.9	−11.0	−7.8	−3.3	−8.4
MNMX-1.0	78.2	17.3	166.4	102.0	35.6	2.0	−16.4	−9.4	−2.9	−2.0
MSD-0.0	75.6	18.8	179.1	101.5	32.8	−1.4	−9.3	−2.5	−3.4	−9.7
MSD-0.5	76.3	17.7	175.8	100.4	32.7	−0.4	−14.6	−4.3	−4.4	−9.9
MCVAR-90%	76.3	18.2	179.0	100.8	33.4	−0.5	−12.4	−2.5	−4.1	−8.0
75th percentile	93.5	23.8	220.9	125.6	63.3	22.0	14.9	20.3	19.5	74.5
90th percentile	85.2	21.0	199.3	113.8	52.2	11.1	1.2	8.5	8.3	43.8
100th percentile	89.2	19.6	200.1	115.8	55.4	16.3	−5.7	8.9	10.3	52.5

- Compared with the one with the average flow pattern, the timing plans resulted from three new models offer similar levels of efficiency, but are much more robust, judging from all perspectives of robustness, i.e., stability of performance, the worst-case performance and average loss against high-consequence scenarios. This demonstrates that the proposed approaches are able to produce more robust timing plans without losing optimality.
- The timing plans optimized using symmetric robustness measure (SD) also leads to improvements with asymmetric measures (worst-case, 90th percentile and 90% CVaR) and vice versa. Moreover, the gains on robustness offered by the proposed models are more significant under the under-saturated condition than the over-saturated condition.
- There exists a tradeoff between efficiency and robustness. The computation experiments confirm that a larger value of γ, α or θ leads to a more robust but less efficient timing plan. The proposed approaches are flexible in representing different preferences traffic engineers may have.
- Simply using one specific percentile of flows to optimize signals may not be sensible. In our experiments, for the under-saturated cases, higher percentiles of flows result in more robust timing plans without losing much efficiency. However, the results are also mixed. 90th percentile plan actually increases both mean and SD. More importantly, when over-saturated, use of higher percentiles of flows actually produces timing plans that are neither robust nor efficient.

To further demonstrate the use of the MNMX model, we conduct another experiment for the situations where traffic engineers do not have enough resources for data collection but instead estimate the likely minimum and maximum flows based on their prior knowledge about the intersection. To reflect their biases, which they are very likely to have, we randomly generate their estimates by assuming the deviations to the "unbiased" minimum and maximum flows reported in Table 1 are independently uniformly distributed between $[-75, 75]$. Table 6 reports only three estimates (randomly generated and selected), for the over-saturated case. Given these estimates, the MNMX model is then used to optimize the timing plans, which are then evaluated using the same Monte-Carlo simulation. Table 6 reports the evaluation results, compared with the one using the true average flow (reported in Table 1). It can be seen that even with biased estimates of minimum and maximum flows, the MNMX approach is able to generate timing plant that performs reasonably well and stably.

5.2. Example 2

The proposed models and algorithms are also applied to a real-world intersection between 164th Street SW and Alderwood Mall Parkway in the City of Lynnwood, Washington. From the video footage recorded in March–April, 2005, 36 observed flow patterns are retrieved for the PM peaks (4:30–6:30 p.m.) between Tuesdays and Thursdays, as reported in Table 7. A phase sequence of (1,5), (2,6), (3,8) and then (4,7) is predetermined for this particular intersection, and the saturation flow rates for lane groups 1–8 are 1650, 3200, 1650, 1700, 1650, 3200, 1650 and 1700, respectively. Other settings, such as loss time and minimum green, are the same as those in Example 1.

The MSD and MCVAR problems are solved against these 36 flow scenarios with γ equal to 0.5 and α equal to 90%, respectively, while the MNMX problem is solved using the maximum and minimum flow scenarios, as reported in Table 7, with θ equal to 0.5. The resulting three robust timing plans are then compared in a similar Monte-Carlo simulation with those generated by using the traditional approach with the average flows, 75th, 90th and 100th percentile flows (reported in Table 7). In the simulation, 5000 samples of traffic flows are drawn from normal distributions with means and SDs reported in Table 7. All the timing plans are reported in Tables 8 and 9 compares the performances of these timing plans, which confirms the observations we have made before. More specifically, based on these 36 scenarios, the MSD and MCVAR models are able to generate timing plans that are less sensitive to the fluctuations in traffic flows (SD decreases by 15.0% and 16.3%,

Table 6
Impacts of specified minimum and maximum flows

Lane group	Case 1			Case 2			Case 3		
	Minimum flow	Maximum flow	Timing	Minimum flow	Maximum flow	Timing	Minimum flow	Maximum flow	Timing
1	137	441	26	29	395	23	133	466	21
2	215	800	18	222	756	18	279	727	19
3	541	1157	28	477	1216	28	488	1128	26
4	215	422	30	133	420	28	143	354	27
5	227	473	18	227	481	18	191	513	19
6	257	1069	26	239	1011	23	278	934	21
7	651	1234	30	530	1193	28	548	1180	27
8	139	367	28	137	312	28	146	400	26
Cycle length	116			112			106		
Mean of delays per vehicle	81.4			77.8			75.9		
SD of delays per vehicle	18.5			17.7			18.2		
Change of mean (%)	7.3			2.6			0.1		
Change of SD (%)	−10.3			−13.9			−11.8		

Table 7
Observed flow scenarios for the PM peak

Scenarios group	Lane group							
	1	2	3	4	5	6	7	8
1	172	968	224	140	56	860	68	384
2	204	932	260	144	40	972	48	376
3	176	1040	284	128	56	1128	52	348
4	248	780	188	88	44	948	40	408
5	220	924	196	144	48	1044	44	344
6	180	928	304	132	64	1252	60	296
7	208	936	296	172	88	1096	88	348
8	172	840	228	168	44	1104	32	388
9	220	1024	324	108	60	948	72	444
10	192	892	220	152	40	1120	56	388
11	232	844	204	148	48	1080	36	372
12	216	1200	280	156	92	976	60	324
13	184	1012	308	132	60	1124	80	420
14	204	944	216	192	64	1084	68	368
15	212	1012	280	148	28	988	92	440
16	212	1040	304	184	52	1048	64	408
17	284	980	248	120	48	1184	60	332
18	168	828	260	160	56	968	68	524
19	220	1108	264	144	96	1092	64	416
20	200	1048	280	184	72	984	60	432
21	268	976	288	152	60	1072	72	384
22	168	1340	312	200	100	1140	72	332
23	232	1040	240	208	84	1068	64	400
24	232	1140	340	196	64	1036	80	384
25	200	1080	348	148	56	1020	60	504
26	196	1072	400	152	84	1092	32	500
27	200	1304	204	180	76	1000	48	372
28	288	916	276	144	80	1028	88	472
29	204	1308	260	132	64	1000	56	448
30	236	1348	248	160	68	1164	52	380
31	192	1092	300	168	84	968	36	548
32	196	948	408	164	76	1032	56	592
33	264	872	216	188	40	1124	44	472
34	240	964	216	152	92	1148	72	524
35	196	948	308	148	48	1112	56	656
36	280	796	228	200	160	1292	40	484
Mean	214	1012	271	157	66	1064	59	423
SD	33	147	53	27	24	89	16	80
Max	288	1348	408	208	100	1252	92	656
Min	168	780	188	88	28	860	32	296
75th percentile	200	1304	204	180	76	1000	48	372
90th percentile	196	948	408	164	76	1032	56	592
100th percentile	280	796	228	200	160	1292	40	484

Table 8
Resulting timing plans

Lane group	1	2	3	4	5	6	7	8	Cycle length
Average	11	31	21	8	11	31	8	21	85
MNMX-0.5	12	35	26	9	12	35	9	26	95
MSD-0.5	12	39	26	9	12	39	9	26	100
MCVAR-90%	12	40	27	8	12	40	8	27	101
75th percentile	11	41	20	9	11	41	9	20	94
90th percentile	10	34	32	8	10	34	8	32	98
100th percentile	16	45	27	11	16	45	11	27	113

respectively) and perform better against the worst-case scenario (the worst-case delay drops by 8.2% and 11.3%, respectively) or high-consequence scenarios (the 90% CVaR of the loss is reduced by 13.8% and 5.3%, respectively) while maintaining the same level of average efficiency (average delay increases by 0.0% and 1.5%, respectively). The MNMX model presents a comparable performance, however, with an increase of CVaR by 9.6%, which should not be surprising since the model does not intend to minimize CVaR in the first place.

Table 9
Comparisons of timing plans via Monte-Carlo simulation

	Mean of delays per vehicle	SD of delays per vehicle	Worst-case delays per vehicle	90th percentile delays per vehicle	90% CVaR of loss	Change (%)				
						Mean	SD	Worst	90th	CVaR
Average	57.0	11.1	117.3	72.1	15.2	–	–	–	–	–
MNMX-0.5	57.7	9.8	111.5	70.6	16.6	1.2	−12.0	−4.9	−2.1	9.6
MSD-0.5	57.0	9.5	107.6	69.7	13.1	0.0	−15.0	−8.2	−3.3	−13.8
MCVAR-90%	57.9	9.3	104.0	70.4	14.4	1.5	−16.3	−11.3	−2.4	−5.3
75th percentile	63.1	14.6	138.2	83.4	28.4	10.7	31.5	17.8	15.7	87.0
90th percentile	68.4	12.6	129.7	85.2	37.2	19.9	13.2	10.6	18.2	145.1
100th percentile	59.2	10.5	119.7	73.7	16.9	3.7	−5.6	2.1	2.3	11.3

6. Conclusion

We have presented three models, MSD, MCVAR and MNMX, respectively, to determine robust optimal timing plans, and demonstrated these models on isolated fixed-time signalized intersections. It has been shown that the proposed models are able to produce timing plans whose performances are less sensitive to fluctuations of traffic flows or perform better against worst-case or high-consequence scenarios without losing optimality. All of these three models are practical, and simple to implement. The models should be chosen to use based on traffic engineers' attitude towards robustness. The min–max approach may be of more practical interest since it requires neither an extensive data collection effort nor a prior knowledge of distributions of traffic flow. The model simply works with engineers' estimates on minimum and maximum possible traffic arrivals. Moreover, the results from the model are not so sensitive to those estimates.

As aforementioned, although we demonstrate these three models on isolated fixed-time signalized intersections, the principles and methodology involved can be applied to deal with more sophisticated signal control systems for intersections, corridors and grid networks. For example, the uncertainty of saturation flow rates can be further addressed for isolated signal control. If a permissive phase exists, the corresponding saturation flow rate may depend on the opposing flow, which can be characterized by an ellipsoidal likelihood region and incorporated into the MNMX model. As another example, the approaches can be applied to synchronize actuated signals along arterials or at grid networks for smooth and stable progression under uncertain traffic conditions. Zhang and Yin (in press) applied the CVaR approach to synchronize actuated signals along arterials, mainly addressing the issue of uncertain (not fixed) starts/ends of green of sync phases. The paper bases the model development on Little's mixed-integer linear programming (MILP) formulation (Little, 1966), which maximizes the two-way bandwidth to synchronize signals along arterials by determining offsets and progress speed adjustment, etc. Little's MILP formulation has been proven to be a flexible and robust approach for signal synchronization and actually lays the foundation for MAXBAND (Messer et al., 1987). It has been later extended to consider variable bandwidth, phase sequencing and grid network synchronization (e.g, Gartner and Stamatiadis, 2002, 2004). Little's formulation assumes that the durations of minor phases (red times of sync phases) are deterministic. Such an assumption does not hold for actuated signal control, where the phase durations of minor phases vary between zero (skipped) and the corresponding maximum greens. By specifying scenarios as realizations of uncertain red times of sync phases, Zhang and Yin (in press) defined the regret associated with a coordination plan with respect to each scenario, and then formulated a robust counterpart of Little's formulation as another MILP to minimize the average regret incurred by a set of high-consequence scenarios. The formulated MILP is easy to solve and the computational time only increases polynomially as the number of scenarios increases. It is demonstrated in a numerical example that the resulting robust coordination plan is able to perform much better against high-consequence scenarios (the worst-case and 90th percentile bandwidths increase by approximately 20%) without losing optimality in average.

Acknowledgements

This research was partly funded by the California Department of Transportation (Caltrans). The contents of this paper reflect the views of the author, who are responsible for the facts and the accuracy of the data presented herein. The contents do not necessarily reflect the official views or policies of the State of California.

The author wishes to thank Kai Leung, Paul Chiu, James Lau and Lindy Cabugao of Caltrans for their continuing cooperation and support during the study. The paper benefits from the discussions with Prof. Alex Skabardonis and Meng Li at California PATH, Profs. Scott Washburn, Lily Elefteriadou and Siriphong Lawphongpanich at University of Florida. The author is also grateful to Prof. Yinhai Wang at University of Washington for providing the data used in one of the numerical examples. Finally the author would like to thank the associate editor, Prof. Benjamin Heydecker, and three anonymous reviewers for their constructive comments that lead to a much improved paper.

References

Bazaraa, M.S., Sherali, H.D., Shetty, C.M., 1993. Nonlinear Programming: Theory and Algorithms, second ed. John Wiley & Sons, New York, NY.
Ben-Tal, A., Nemirovski, A., 1999. Robust solutions to uncertain linear programs. Operations Research Letters 25 (1), 1–13.
Ben-Tal, A., Nemirovski, A., 2002. Robust optimization – methodology and applications. Mathematical Programming Series B 92 (3), 453–480.

Chen, G., Daskin, M.S., Shen, Z.J.M., Uryasev, S., 2006. The α-reliable mean-excess regret model for stochastic facility location modeling. Naval Research Logistics 53 (7), 617–626.
Dion, F., Rakha, H., Kang, Y-S., 2004. Comparison of delay estimates at under-saturated and over-saturated pre-timed signalized intersections. Transportation Research Part B 38 (2), 99–122.
Gazis, D.C., 1964. Optimum control of a system of oversaturated intersections. Operations Research 12 (6), 815–831.
Gartner, N.H., 2002. Development and implementation of an adaptive control strategy in a traffic signal network: the virtual-fixed-cycle approach. In: Taylor, A.P. (Ed.), Transportation and Traffic Theory in the 21st Century: Proceedings of the 15th International Symposium on Transportation and Traffic Theory. Pergamon, pp. 137–155.
Gartner, N.H., Stamatiadis, C., 2002. Arterial-based control of traffic flow in urban grid networks. Mathematical and Computer Modeling 35 (5-6), 657–671.
Gartner, N.H., Stamatiadis, C., 2004. Progression optimization featuring arterial- and route-based priority signal networks. ITS Journal 8 (2), 77–86.
Heydecker, B., 1987. Uncertainty and variability in traffic signal calculations. Transportation Research Part B 21 (1), 79–85.
Laguna, M., 1998. Applying robust optimization to capacity expansion of one location in telecommunications with demand uncertainty. Management Science 44 (11), 101–110.
Little, J.D.C., 1966. The synchronization of traffic signals by mixed-integer linear programming. Operations Research 14 (4), 568–594.
Luyanda, F., Gettman, D., Head, L., Shelby, S., Bullock, D., Mirchandani, P., 2003. ACS-Lite algorithmic architecture: applying adaptive control system technology to closed-loop traffic signal control systems. Design guidelines for deploying closed loop systems. Transportation Research Record 1856, 175–184.
Krokhmal, P., Palmquist, J., Uryasev, S., 2002. Portfolio optimization with conditional value-at-risk objective and constraints. Journal of Risk 4 (2), 43–68.
Messer, C.J., Hogg, G.L., Chaudhary, N.A., Chang, E., 1987. Optimization of Left Turn Phase Sequence in Signalized Networks using MAXBAND 86, Summary Report, vol. 1. Technical Report FHWA/RD-87/109, FHWA, Washington, DC.
Mulvey, J.M., Vanderbei, R.J., Zenios, S.A., 1995. Robust optimization of large-scale systems. Operations Research 43 (2), 264–281.
National Electrical Manufacturers Association, 1989. NEMA TS 1 Traffic Control Systems.
Ribeiro, P.C.M., 1994. Handling traffic fluctuation with fixed-time plans calculated by TRANSYT. Traffic Engineering and Control 35 (6), 362–366.
Rockafellar, R.T., Uryasev, S., 2002. Conditional value-at-risk for general loss distribution. Journal of Banking and Finance 26 (7), 1443–1471.
Robertson, D.I., Bretherton, R.D., 1991. Optimizing networks of traffic signals in real-time: the SCOOT method. IEEE Transactions on Vehicular Technology 40 (1), 11–15.
Smith, B.L., Scherer, W.T., Hauser, T.A., Park, B.B., 2002. Data-driven methodology for signal timing plan development: a computational approach. Computer-Aided Civil and Infrastructure Engineering 17 (6), 387–395.
TRB Committee on Highway Capacity and Quality of Service, 2000. Highway Capacity Manual.
Vincent, R.A., Mitchell, A.I., Roberson, D.I., 1980. User Guide to TRANSYT Version 8. TRRL Report LR888, Transport and Road Research Laboratory, Crowthorne.
Wallace, C.E., Courage, K.G., Hadi, M.A., Gan, A.G., 1998. TRANSYT-7F User's Guide. University of Florida, Gainesville, FL.
Webster, F.V., 1958. Traffic Signal Settings, Road Research Technical Paper No. 39. Her Majesty's Stationery Office.
Yin, Y., in press. A scenario-based model for fleet allocation of freeway service patrols. Network and Spatial Economics.
Yin, Y., Lawphongpanich, S., 2007. A robust approach to the continuous network design problem with demand uncertainty. In: Allsop, R.E., Bell, M.G.H., Heydecker, B.G. (Eds.), Transportation and Traffic Theory 2007: Papers Selected for Presentation at ISTTT17, A Peer Reviewed Series Since 1959. Elsevier, pp. 111–126.
Zhang, L., Yin, Y., in press. Robust synchronization of actuated signals on arterials. Transportation Research Record.